

GENERALIZATION OF THE HOFMANN-ZOTTER COMBINED-FUNCTION FORMULATION FOR APPLICATION TO 50x50 GeV e<sup>+</sup>e<sup>-</sup> STORAGE RINGS\*

L. E. Sakazaki and R. M. Talman  
Newman Laboratory of Nuclear Studies  
Cornell University  
Ithaca, NY 14853

Summary

Though all existing strong-focusing electron storage rings have separated-function lattices, the combined-function lattice would reduce energy loss to synchrotron radiation. Robinson<sup>1</sup> and Hofmann and Zotter<sup>2</sup> have shown how to overcome the anti-damping that was once thought to rule out this possibility. Their formulation is generalized to achieve a more realistic machine design having FODO cells to incorporate the inevitable straight sections between magnets and to allow for any subsequent insertion of nonlinear elements. An analysis is performed to estimate the energy savings for a 50x50 GeV e<sup>+</sup>e<sup>-</sup> facility using combined-function magnets.

Introduction

The advantages of the combined-function over the separated-function lattice in the design of strong-focusing electron storage rings are a reduction in energy loss to synchrotron radiation and a reduction in the total number of magnets. Because the synchrotron radiation energy loss is proportional to the fourth power of the beam energy and to the inverse of the average bending radius, maximization of the bending radius is desirable with very high beam energies. The combined-function lattice achieves a larger bending radius by housing bending and focusing effects in a single unit rather than in separate magnets, thereby distributing the total bend of 2π radians over a larger fraction of the storage ring.

A key step in the design of a combined-function lattice is to insure that the horizontal betatron oscillations are damped, by making the defocusing magnets stronger than the focusing ones. This technique was suggested by Robinson<sup>1</sup> and has been implemented by Hofmann and Zotter<sup>2</sup> in their combined-function FD (focusing-defocusing) lattice formulation. In this paper we extend the combined-function FD formalism to the FODO (focusing-straight-defocusing-straight) lattice, so that combined-function machine parameters can be evaluated for a realistic accelerator design. Main results are presented here, while more detailed calculations are given elsewhere.<sup>3</sup>

Combined-Function FODO Lattice Synchrotron Radiation Integrals

The synchrotron radiation integrals<sup>2,4</sup>,

$$\begin{aligned} I_1 &\equiv \oint G(s)\eta(s)ds \\ I_2 &\equiv \oint G^2(s)ds \\ I_3 &\equiv \oint G^3(s)ds \\ I_4 &\equiv \oint G(s)[G^2(s) \pm 2K(s)]\eta(s)ds \\ I_5 &\equiv \oint G^3(s)\mathcal{H}(s)ds, \end{aligned} \quad (1)$$

appear in the calculation of the momentum compaction, synchrotron radiation energy loss, beam sizes, and horizontal betatron oscillation damping. As applied to the combined-function lattice, these integrals become

$$\begin{aligned} I_1 &= N \left( \frac{L_F}{\rho_F} \langle \eta_F \rangle + \frac{L_D}{\rho_D} \langle \eta_D \rangle \right) \\ I_2 &= N \left( \frac{L_F}{\rho_F^2} + \frac{L_D}{\rho_D^2} \right) \\ I_3 &= N \left( \frac{L_F}{\rho_F^3} + \frac{L_D}{\rho_D^3} \right) \\ I_4 &\approx 2N \left( \frac{L_F K_F}{\rho_F} \langle \eta_F \rangle - \frac{L_D K_D}{\rho_D} \langle \eta_D \rangle \right) \\ I_5 &= N \left( \frac{L_F}{\rho_F^3} \langle \mathcal{H}_F \rangle + \frac{L_D}{\rho_D^3} \langle \mathcal{H}_D \rangle \right). \end{aligned} \quad (2)$$

N is the number of FODO cells. Focusing and defocusing magnet lengths are L<sub>F</sub> and L<sub>D</sub>, bending radii are ρ<sub>F</sub> and ρ<sub>D</sub>, and focusing strengths are K<sub>F</sub> and K<sub>D</sub>.

"Curly  $\mathcal{H}$ ", defined by

$$\mathcal{H} = \frac{\eta^2}{\beta} + \beta(\eta' - \frac{\beta'}{2\beta}\eta)^2, \quad (3)$$

where β is the betatron function and η is the dispersion function, is a relative of the Courant-Snyder invariant. After a somewhat lengthy calculation, we find the average values

$$\begin{aligned} \langle \mathcal{H}_F \rangle &= \frac{1}{K_F \rho_F^2} \left[ (A_F^* - B_F^*) \left( 1 + 2E_F \frac{\sin x_F}{x_F} + E_F^2 \right) \right. \\ &\quad \left. + B_D^* \left( \frac{\sinh 2x_D}{2x_D} - 1 \right) \right] \\ \langle \mathcal{H}_D \rangle &= \frac{1}{K_D \rho_D^2} \left[ (B_D^* - A_D^*) \left( 1 - 2E_D \frac{\sinh x_D}{x_D} + E_D^2 \right) \right. \\ &\quad \left. + B_F^* \left( 1 - \frac{\sin 2x_F}{2x_F} \right) \right] \end{aligned} \quad (4)$$

and

$$\begin{aligned} \langle \eta_F \rangle &= \frac{1}{K_F \rho_F} \left( E_F \frac{\sin x_F}{x_F} + 1 \right) \\ \langle \eta_D \rangle &= \frac{1}{K_D \rho_D} \left( E_D \frac{\sinh x_D}{x_D} - 1 \right), \end{aligned} \quad (5)$$

where

$$\begin{aligned} A_F^* &= \frac{1}{\sqrt{K_F} \sin \mu} \left[ sC - \frac{1-p^2}{2p} cS + (\sqrt{K_F} cC + \sqrt{K_D} sS)L_0 \right. \\ &\quad \left. + \frac{1}{2} \sqrt{K_F K_D} cSL_0^2 \right] \\ B_F^* &= \frac{1}{\sqrt{K_F} \sin \mu} \left( \frac{1+p^2}{2p} sS + \sqrt{K_F} cL_0 + \frac{1}{2} \sqrt{K_F K_D} sL_0^2 \right) \end{aligned}$$

\*Work supported by the National Science Foundation.

$$\begin{aligned}
A_D^* &= \frac{1}{\sqrt{K_D} \sin \mu} \left[ cS + \frac{1-p^2}{2p} sC + (\sqrt{K_D} cC - \sqrt{K_F} sS) L_0 \right. \\
&\quad \left. - \frac{1}{2} \sqrt{K_F K_D} sC L_0^2 \right] \\
B_D^* &= \frac{1}{\sqrt{K_D} \sin \mu} \left( \frac{1+p^2}{2p} s + \sqrt{K_D} cL_0 - \frac{1}{2} \sqrt{K_F K_D} sL_0^2 \right) \\
E_F &= (1+rp^2) \frac{\sinh x_D}{\text{Den} + L_0 \sqrt{K_F} \sin x_F \sinh x_D} \\
E_D &= \frac{1+rp^2}{rp} \frac{\sin x_F}{\text{Den} + L_0 \sqrt{K_F} \sin x_F \sinh x_D}
\end{aligned} \quad (6)$$

with

$$\begin{aligned}
x_F &\equiv \frac{L_F}{2} \sqrt{K_F} \quad , \quad x_D \equiv \frac{L_D}{2} \sqrt{K_D} \quad , \\
q &\equiv \frac{L_F}{L_D} \quad , \quad r \equiv \frac{\rho_F}{\rho_D} \quad , \quad p \equiv \sqrt{\frac{K_F}{K_D}} \quad , \\
c &\equiv \cos 2x_F \quad , \quad C \equiv \cosh 2x_D \quad , \\
s &\equiv \sin 2x_F \quad , \quad S \equiv \sinh 2x_D \quad , \\
\text{Den} &\equiv p \sin x_F \cosh x_D - \cos x_F \sinh x_D \quad .
\end{aligned} \quad (7)$$

Each of the two straight sections of a FODO cell has length  $L_0$ .  $\mu$  is the phase shift per FODO cell. The subscript F denotes horizontal focusing (and vertical defocusing), while the subscript D stands for horizontal defocusing (and vertical focusing).

#### Magnet Lengths, Bending Radii, and Focusing Strengths

To determine the six parameters  $L_F$ ,  $L_D$ ,  $\rho_F$ ,  $\rho_D$ ,  $K_F$ , and  $K_D$ , we impose six design restrictions.

#### Damping of Betatron and Energy Oscillations

The damping partition numbers are<sup>4</sup>

$$J_x = 1 - \frac{I_4}{I_2} \quad , \quad J_z = 1 \quad , \quad J_E = 2 + \frac{I_4}{I_2} \quad . \quad (8)$$

For damping of betatron and energy oscillations,  $J_x$ ,  $J_z$ , and  $J_E$  all must be positive. Because  $J_x + J_E = 3$ , we must have  $0 < J_x < 3$  ( $3 > J_E > 0$ ) for damping. Using Eqs. (2), (5), (6), and (7) in Eq. (8), we arrive at the damping condition

$$\frac{2}{J_x + 1} (r-1) \frac{1+rp^2}{1+\frac{r^2}{q}} \frac{\sin x_F \sinh x_D}{x_F (\text{Den} + L_0 \sqrt{K_F} \sin x_F \sinh x_D)} = 1 \quad , \quad (9)$$

with  $0 < J_x < 3$ . This condition implies that  $r = \rho_F/\rho_D > 1$ , i.e., the defocusing magnets must be stronger than the focusing magnets to overcome anti-damping.

#### Horizontal and Vertical Phase Shifts

The phase shift in the horizontal plane,  $\mu_H$ , is obtained by taking one-half of the trace of the FODO transfer matrix

$$M(s + L_{\text{FODO}}, s) = \text{ODOF}$$

$$= \begin{pmatrix} 1 & L_0 \\ 0 & 1 \end{pmatrix} \begin{pmatrix} c & \frac{1}{\sqrt{K_D}} s \\ \sqrt{K_D} s & c \end{pmatrix} \begin{pmatrix} 1 & L_0 \\ 0 & 1 \end{pmatrix} \begin{pmatrix} c & \frac{1}{\sqrt{K_F}} s \\ -\sqrt{K_F} s & c \end{pmatrix} \quad . \quad (10)$$

We find

$$\begin{aligned}
\cos \mu &= \cos \mu_H = \cos 2x_F \cosh 2x_D + \frac{1-p^2}{2p} \sin 2x_F \sinh 2x_D \\
&\quad + (\sqrt{K_D} \cos 2x_F s \sinh 2x_D - \sqrt{K_F} \sin 2x_F \cosh 2x_D) L_0 \\
&\quad - \frac{1}{2} \sqrt{K_F K_D} \sin 2x_F \sinh 2x_D L_0^2 \quad . \quad (11)
\end{aligned}$$

Also, by requiring  $\mu_H = \mu_V$  and taking the trace of the matrix  $M = \text{OFOD}$ , we arrive at an expression for the phase shift in the vertical plane,

$$\begin{aligned}
\cos \mu &= \cos \mu_V = \cos 2x_D \cosh 2x_F - \frac{1-p^2}{2p} \sin 2x_D \sinh 2x_F \\
&\quad + (\sqrt{K_F} \cos 2x_D \sinh 2x_F - \sqrt{K_D} \sin 2x_D \cosh 2x_F) L_0 \\
&\quad - \frac{1}{2} \sqrt{K_F K_D} \sin 2x_D \sinh 2x_F L_0^2 \quad . \quad (12)
\end{aligned}$$

#### Full and Closed Ring

Neglecting long straight sections, RF cavities, interaction regions, etc., we require that our model combined-function storage ring consist entirely of FODO cells with the "fullness" condition

$$C_{\text{arc}} = N(L_F + L_D + 2L_0) \quad . \quad (13)$$

Yet another requirement is the "closure" condition that the total bending angle be  $2\pi$  radians,

$$2\pi = N \left( \frac{L_F}{\rho_F} + \frac{L_D}{\rho_D} \right) \quad . \quad (14)$$

#### Special Case

The sixth and final restriction is one of two special case requirements: either (a) equal length focusing and defocusing magnets ( $L_F = L_D$ ), or (b) equal profile parameters in the focusing and defocusing magnets ( $\rho_F K_F = \rho_D K_D$ ). The special case requirement, together with Eqs. (9), (11), (12), (13) and (14), completely determines the magnet lengths, bending radii, and focusing strengths, once the input design parameters  $C_{\text{arc}}$ ,  $N$ ,  $\mu$ ,  $L_0$ , and  $J_x$  are specified.

#### Combined-Function Magnet Design

With  $L_F$ ,  $L_D$ ,  $\rho_F$ ,  $\rho_D$ ,  $K_F$ ,  $K_D$ , and the synchrotron radiation integrals (2) all determined, we proceed to calculate the combined-function magnet pole profiles. The maximal horizontal and vertical rms beam sizes are given by

$$\begin{aligned}
\hat{\sigma}_x^2 &= \hat{\sigma}_{x\beta}^2 + \hat{\sigma}_{x\varepsilon}^2 = \frac{\sigma_{x\beta}^2}{B} \hat{\beta} + \left( \frac{\sigma_{x\varepsilon}}{E} \right)^2 \hat{\eta}^2 \\
\hat{\sigma}_z^2 &= \hat{\sigma}_{z\beta}^2 = \frac{1}{2} \hat{\sigma}_{x\beta}^2 \quad ,
\end{aligned} \quad (15)$$

where<sup>4</sup>

$$\frac{\sigma_{x\beta}^2}{B} = \frac{C_q}{J_x} \gamma_0^2 \frac{I_5}{I_2} \quad , \quad \left( \frac{\sigma_{x\varepsilon}}{E} \right)^2 = \frac{C_q}{3-J_x} \gamma_0^2 \frac{I_3}{I_2} \quad , \quad (16)$$

$$\hat{\beta} = A_F^* + B_F^* \quad , \quad \hat{\eta} = \frac{1}{K_F \rho_F} (E_F + 1) \quad ,$$

with

$$\begin{aligned}
C_q &\equiv \frac{55}{32\sqrt{3}} \frac{h}{mc} \approx 3.83194 \times 10^{-13} \text{ m} \\
\gamma_0 &\equiv \frac{E}{mc^2} \approx \frac{10^3}{0.511003} E \quad (E \text{ in GeV}) \quad . \quad (17)
\end{aligned}$$

$E$  is the energy per beam. The horizontal and vertical full apertures are<sup>2</sup>

$$A_H = 2 \cdot (6+4) \hat{\delta}_x + \text{c.o.} = 20 \hat{\delta}_x + \text{c.o.}$$

$$A_V = 2 \cdot 6 \hat{\delta}_z + \text{c.o.} = 12 \hat{\delta}_z + \text{c.o.}, \quad (18)$$

where c.o. is the closed orbit uncertainty (taken to be about 10 mm).

The faces of the focusing and defocusing combined-function magnets (which may be viewed as half-quadrupoles) are equipotential hyperbolic surfaces having pole profile equations

$$\left( \frac{\rho_F}{|n_F|} + x \right) z = \pm \frac{\rho_F}{|n_F|} z_{oF}$$

$$\left( \frac{\rho_D}{n_D} - x \right) z = \pm \frac{\rho_D}{n_D} z_{oD}, \quad (19)$$

with field indices

$$n_F = -\rho_F^2 K_F < 0, \quad n_D = +\rho_D^2 K_D > 0, \quad (20)$$

and

$$z_{oF} = \left[ 1 + \frac{|n_F|}{\rho_F} \frac{A_H}{2} \right] \frac{A_V}{2}$$

$$z_{oD} = \left[ 1 + \frac{n_D}{\rho_D} \frac{A_H}{2} \right] \frac{A_V}{2}. \quad (21)$$

Fig. 1 shows the pole profiles of F and D combined-function magnets.

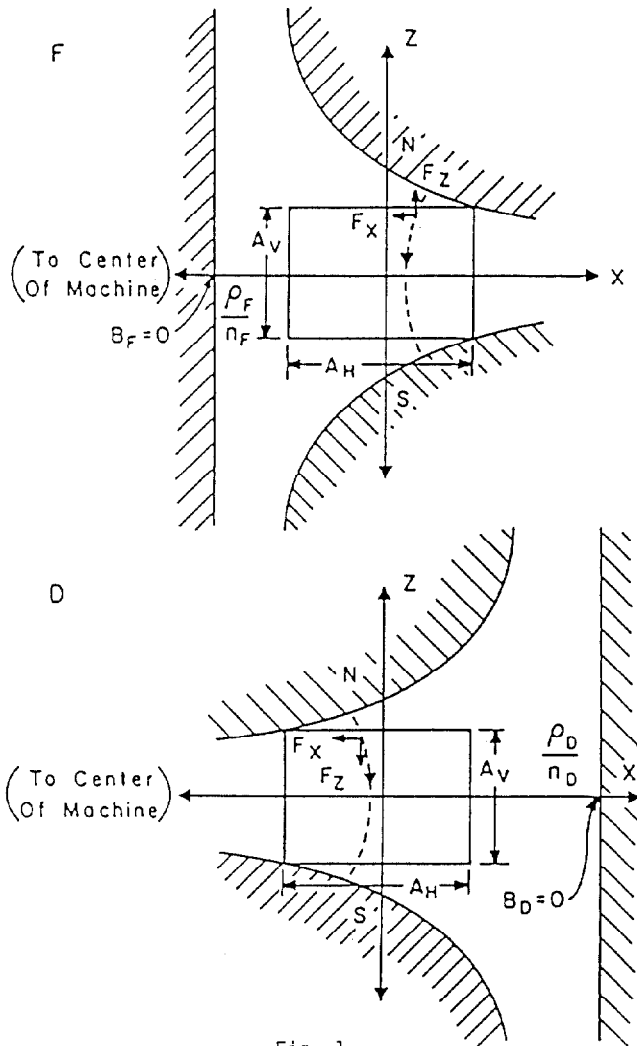


Fig. 1

### Energy Savings

The synchrotron radiation energy loss per turn is

$$U_o = \frac{C_Y E^4}{2\pi} I_2, \quad (22)$$

where

$$C_Y = \frac{4\pi}{3} \frac{r_e}{(mc^2)^3} = 8.84606 \times 10^{-5} \text{ m}/(\text{GeV})^3.$$

While the integral  $I_2$  is evaluated exactly in Eq. (2), to good approximation we make the estimate

$$I_2 = \int G^2(s) ds \approx \frac{2\pi}{\langle \rho \rangle} = \frac{2\pi}{F_m R_{\text{arc}}} \quad (23)$$

where  $R_{\text{arc}} = C_{\text{arc}}/2\pi$  and  $F_m$  is the bending magnet fill factor ( $0 < F_m < 1$ ).

Typical half-cells of separated-function and combined-function lattices are shown in Fig. 2.

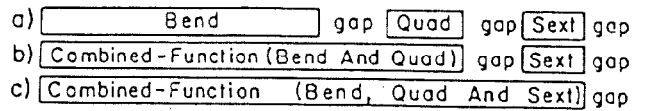


Fig. 2

For a 50x50 GeV e<sup>+</sup>e<sup>-</sup> machine with arc circumference  $C_{\text{arc}} = 4335$  m and  $N = 240$  cells, to be specific, fill factors for the designs in Fig. 2a,b,c are  $(F_m)_{\text{sep}} = .72$ ,  $(F_m)_{\text{comb}} = .86$ , and  $(F_m)_{\text{comb}} = .91$ , respectively. The percent energy savings of a combined-function lattice over a separated-function lattice is then

$$\frac{(U_o)_{\text{sep}} - (U_o)_{\text{comb}}}{(U_o)_{\text{sep}}} = \frac{(I_2)_{\text{sep}} - (I_2)_{\text{comb}}}{(I_2)_{\text{sep}}} \approx 1 - \frac{(F_m)_{\text{sep}}}{(F_m)_{\text{comb}}} \approx 15 \text{ to } 20\%. \quad (24)$$

Our exact results for this machine, using calculations outlined in this paper, yield energy savings of the same order.

### Conclusion

The combined-function lattice, discussed earlier by Hofmann and Zotter<sup>4</sup>, offers a viable alternative to the standard separated-function design of strong-focusing electron storage rings. The main advantage is a predicted 15 to 20% energy savings, corresponding to a reduction in synchrotron radiation energy loss, for a typical 50x50 GeV e<sup>+</sup>e<sup>-</sup> machine. A further advantage is a reduction in the total number of magnets. The combined-function FODO lattice described herein allows one to proceed with the design of a realistic combined-function machine.<sup>5</sup>

### References

1. K.W. Robinson, Phys. Rev. 111, 373 (1958).
2. A. Hofmann and B. Zotter, IEEE Trans. Nucl. Sci. NS-24, No. 3, 1875 (1977), and CERN/ISR-GS/76-28 (1976).
3. L. Sakazaki and R. Talman, CBN 82-31, Cornell Internal Report (1982).
4. M. Sands, SLAC Report 121 (1970).
5. R. Siemann, Cornell Internal Report, in preparation.